

UDC: 538.9 Condensed matter Physics, Solid state Physics, Theoretical Condensed matter Physics

## EFFECT OF ANNEALING ON SOME PHYSICAL PROPERTIES OF COPPER SULFIDE THIN FILMS

Noora Jassim Mohammed

Ministry of Education: Al-Rusafa Third Directorate of Education, Baghdad, Iraq

### Abstract

*Copper sulfide ( $\text{Cu}_2\text{S}$ ) nanostructured thin films were synthesized by chemical bath deposition. The impact of annealing temperature (R.T, 100 and 200 °C) on their structural, electrical, and optical characteristics was investigated. Field-emission scanning electron microscopy (FESEM) and X-ray diffraction (XRD) were used to examine the thin films' structure. FESEM analysis results showed that the produced thin-film nanostructures had nanoparticle diameters ranged within 118.16–26.77 nm. XRD measurements revealed that the amorphous thin films acquired polycrystalline nanostructures after annealing. Electrical measurements showed that the electrical conductivity of the  $\text{Cu}_2\text{S}$  thin films was about 1.64 S/cm, which increased to 3.38 S/cm after annealing at 200 °C. As regards their optical properties, they showed a large absorption in the visible region, with absorption coefficient values of about  $10^4 \text{ cm}^{-1}$ .*

*Key words:*  $\text{Cu}_2\text{S}$  nanostructured, thin films, chemical bath deposition.

### 1.Introduction

$\text{Cu}_x\text{S}$  is a semiconducting compound belonging to the p-type I–VI group.  $\text{Cu}_x\text{S}$  has been eliciting research attention since the discovery of chalcogenide CdS/ $\text{Cu}_x\text{S}$  heterojunction solar cells, which attracting considerable attention [1]. Other uses for  $\text{Cu}_x\text{S}$  compounds include microwave shielding, electrically conductive electrodes, solar-control coatings, laminated glazing, photothermal conversion [2], and photovoltaic and photodetection applications. The electrical conductivity of  $\text{Cu}_x\text{S}$  thin films relies on various film-growth factors, including impurity concentration, film composition, and film thickness, among others [3-4].

The importance of the physical properties of any material is determined by the nature of its use. According to literature, the dominant use of copper sulfide ( $\text{Cu}_2\text{S}$ ) is in the manufacture of solar cells in conjunction with cadmium sulfide.  $\text{Cu}_2\text{S}$  is used as a window through which incident light passes. Thus, studying the optical properties of this material can determine its absorption properties particularly its absorption coefficient [5,6].

The electrical properties of  $\text{Cu}_2\text{S}$  films vary owing to the great dependence of electrical resistance on the chemical equilibrium (copper-to-sulfur ratio) and on changes in particle size and thickness.  $\text{Cu}_2\text{S}$  films are generally electron acceptors owing to their copper vacancies. Hole concentration reportedly decreases with increased copper proportion [7,8].

The characteristics of  $\text{Cu}_x\text{S}$  thin films are affected by their precise stoichiometry, which is determined by the thin film deposition's preparative conditions.  $\text{Cu}_x\text{S}$  thin films are gaining considerable interest owing to their wide-ranging potential applications, including photovoltaic technology. The active layer of photovoltaic cells (e.g.,  $\text{Cd}_{1-y}\text{Zn}_y\text{S}/\text{Cu}_x\text{S}$  cells) is the  $\text{Cu}_x\text{S}$  film [2-9]. Another application is the photothermal conversion of solar energy, wherein  $\text{Cu}_x\text{S}$  films act as a solar absorbent coating such as in selective radiation filters on architectural windows. The films control solar transmittance by depositing electrically conductive coatings onto polymeric substrates. Notably, the low operating temperature for sensor application achieved

when using  $\text{Cu}_x\text{S}$  as a sensor material is the most apparent advantage [10].

The present work aimed to study the morphology, X-ray diffraction (XRD) patterns, optical properties, and electrical conductivity of  $\text{Cu}_2\text{S}$  thin films and to determine the effect of annealing on the these properties of the thin films.

## 2. Experimental

$\text{Cu}_2\text{S}$  thin films were produced by chemical bath deposition (CBD). Double-distilled water was used as the solvent to prepare the required films. Glass slides were fixed vertically inside a beaker, and four components were mixed in a 50 mL beaker, namely, 25 mL of thiourea (0.6 M) and 25 mL of  $\text{CuCl}_2 \cdot 2\text{H}_2\text{O}$  (0.4 M). After adding five to six drops of triethanolamine with stirring, 30%  $\text{NH}_3$  solution added dropwise until pH 11 was reached. All components were subjected to steady magnetic stirring for 1 h with subsequent heat processing at 50 °C. After the deposition process, glass slides (films) were withdrawn from the solution, rinsed with distilled water, and left to dry. Then, the films were annealed at different temperatures ( $T_a = \text{R.T}$ , 100 and 200 °C). The crystalline structure of the  $\text{Cu}_2\text{S}$  nanostructure was investigated through XRD measurements performed at ambient temperature using a PhillipsXpert (Holland). The thin films were imaged with a FESEM system (Tescan Mira3, France). The important optical measurements of absorbance and transmittance were made using an Optima Sp-3000 Plus UV-Vis spectrophotometer.

## 3. Results and Discussion

Figure (1) depicts the FESEM of the  $\text{Cu}_2\text{S}$  thin films at various annealing temperatures. We observed that the surfaces of the thin films grew nanoparticles with diameters up to 118.16 nm, in addition to some irregularly distributed clusters. This morphology changed clearly after annealing, i.e., the diameters of the formed nanoparticles decreased to 31.54 and 26.77 nm at  $T_a = 100$  and 200 °C, respectively. Moreover, the surface of thin films became more regular after annealing. The uniformity in the surfaces of the films and the decrease in nanoparticle sizes indicated an improvement in the structural properties after annealing.

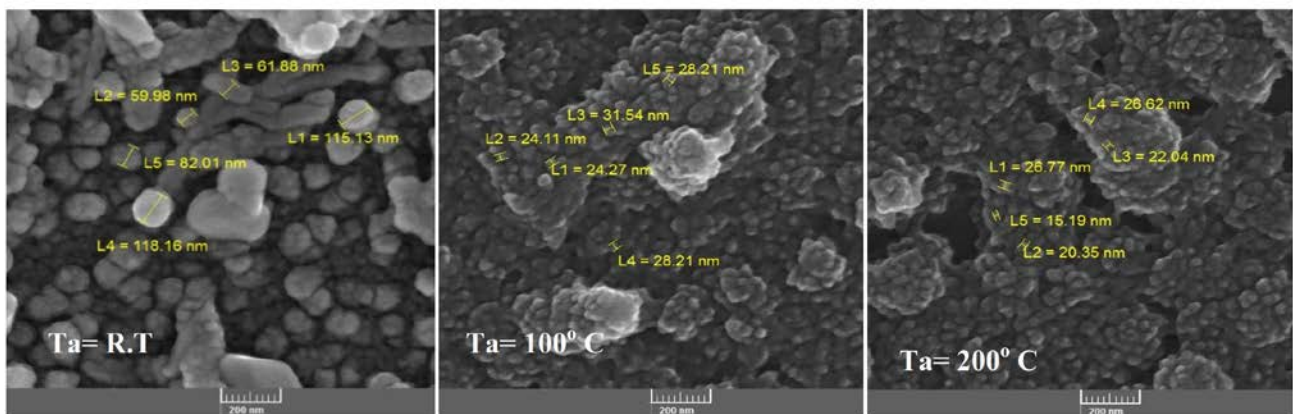


**Figure 1:** FESEM images for the  $\text{Cu}_2\text{S}$  thin films at different annealing temperature.

The XRD patterns of  $\text{Cu}_2\text{S}$  thin films were obtained using an X-ray diffractometer at room temperature. They were matched with (JCPDS) files to ensure that the structure matched the standard  $\text{Cu}_2\text{S}$  structure. The structure analysis and properties of  $\text{Cu}_2\text{S}$  thin films were confirmed by XRD, as shown in figure (2). The XRD spectrum of as-deposited  $\text{Cu}_2\text{S}$  thin films indicated an amorphous structure with no peaks observed in the spectrum. This result is expected for films prepared by chemical bath method [11]. In the same figure, the XRD pattern of  $\text{Cu}_2\text{S}$  thin films at

different annealing temperatures (100 and 200 °C) revealed that the films' crystallinity started to appear after the growth of new peaks at  $2\theta = 30^\circ$  and  $33^\circ$  with annealing, and the number and intensity of peaks increased with increased annealing temperature. This finding indicated an improvement in the crystal structure of the films prepared with annealing. The average grain size of  $\text{Cu}_2\text{S}$  was calculated by Scherer's formula [12], which was about 68.01 nm at  $T_a = 100^\circ\text{C}$  and increased to 82.34 nm at  $T_a = 200^\circ\text{C}$ .

Table 1 shows the change in electrical conductivity in terms of the change in annealing temperature. The table also shows that the electrical conductivity increased with increased annealing temperature, revealing that annealing improved the electrical properties. Through measurements of changes in electrical conductivity with temperature, the films were found to have more than one activation energy, and the value of activation energy changed with the change in annealing temperature. By applying the relationship [13]:-

$$\sigma = \sigma_0 e^{\frac{-E_a}{2KT}} \tag{1}$$

where  $\sigma$  is the conductivity at a temperature change,  $\sigma_0$  : conductivity at room temperature,  $E_a$  : activation energy,  $K$  : Boltzmann constant, and  $T$  is the temperature  
 The change in electrical conductivity was plotted in terms of the reciprocal temperature, as shown in figure 3. Table 1 shows that the activation energies decreased with increased annealing temperature. The increase in conductivity and decrease in activation energy with  $T_a$  may be attributed to the change in structure and state of the films, as well as to the rearrangement of atoms on the substrate surface [14].

TABLE 1 Effect of annealing temperatures on parameters of the  $\text{Cu}_2\text{S}$  thin films.

$T_a$ °C	C.S. nm	$\sigma$ S.cm <sup>-1</sup> ×10 <sup>-7</sup>	$E_{a1}$ eV	$E_{a2}$ eV
R.T	68.01	1.64	0.805	0.082
100	73.50	2.34	0.721	0.084
200	82.34	3.38	0.433	0.072

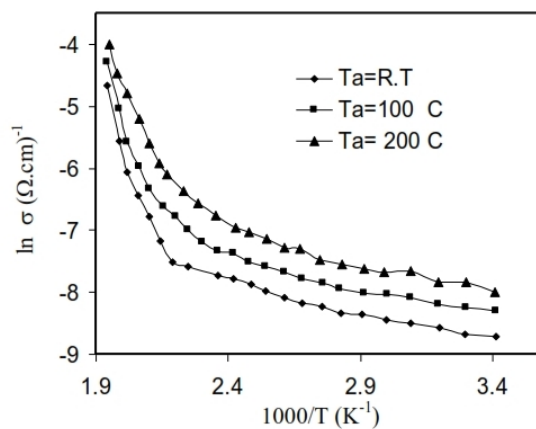


Figure 3: The variation of  $\ln \sigma$  as a function of  $1000/T$  for  $\text{Cu}_2\text{S}$  thin films .

Absorption measurements were performed within 380–900 nm wavelength for as-deposited and annealed Cu<sub>2</sub>S thin films, and results are shown in figure (4). The prepared films were characterized by high absorbance at short wavelengths and then decreased with increased  $\lambda$ . This result signified that the incident photon was unable to irritate the electron and moved it from the valence to the conduction band because the incident photon's energy was smaller than the value of the semiconductor's energy gap. Consequently, absorbance decreased with increased wavelength [15]. Absorption also decreased with increased annealing. The transmittance spectrum, as shown in figure (5), indicated an opposite behavior to the absorbance as the deposited and annealing Cu<sub>2</sub>S thin films were the least possible at the basic absorption edge (short wavelengths). Furthermore, transmittance increased with increased wavelength and then stabilized at 650 nm wavelength in the visible and near-infrared regions.

The absorption coefficient is calculated from the relationship [16]

$$\alpha = 2.303 (A/t) \quad (2)$$

where A, t are the absorption and thickness of thin films respectively.

Figure (6) shows the relation between the absorption coefficient as a function of the incident photon energy for as-deposited and annealed Cu<sub>2</sub>S thin films. The same behavior was observed for all samples, i.e., the absorption coefficient was low at low photon energies. This finding may be due to the low electronic-transition probability, and the  $\alpha$  values increased at the basic absorption edge toward high photon energies. The value of  $\alpha$  was higher than  $10^4 \text{ cm}^{-1}$ , indicating that direct electronic transitions were allowed [17]. As for the annealing, the absorption coefficient increased with increased annealing temperature owing to the effect of annealing on the crystal structure of the prepared films.

The refractive index was calculated according to the relationship [18] :

$$n = \left[ \frac{4R}{(R-1)^2} - k^2 \right]^{1/2} - \frac{(R+1)}{(R-1)} \quad (3)$$

Where R is reflectivity and k extinction coefficient.

Figure (7) represents the change in n as a function of the photon energy for as-deposited and annealing Cu<sub>2</sub>S thin films. The behavior of the refractive index curve for all films was almost constant with increased photon energy until 2 eV. It then decreased within the range of energies corresponding with the basic absorption edge (high photon energies). Meanwhile, the refractive index gradually increased with increased annealing temperature, which was owing to the decrease in reflectivity values and enhancement in structure upon annealing.

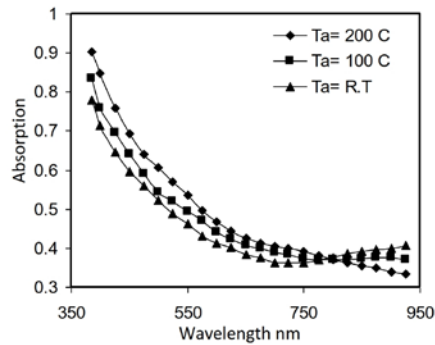


Figure 4: The variation of absorption with wavelength of  $\text{Cu}_2\text{S}$  thin films.

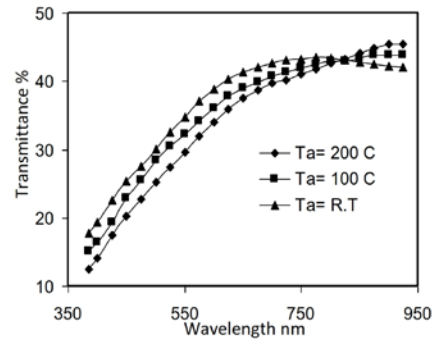


Figure 5: The variation of transmittance with wavelength of  $\text{Cu}_2\text{S}$  thin films.

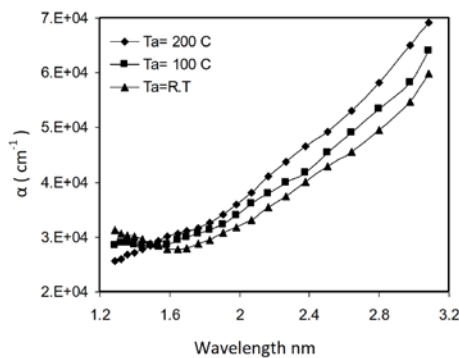


Figure 6: The variation of  $\alpha$  with photon energy of  $\text{Cu}_2\text{S}$  thin films.

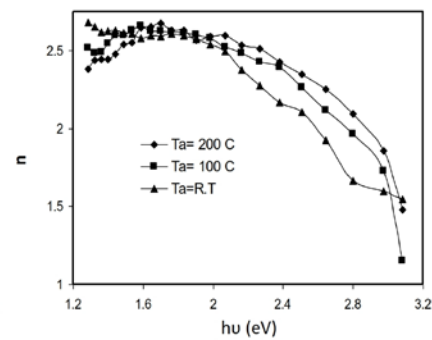


Figure 7: The variation of refractive index with photon energy of  $\text{Cu}_2\text{S}$  thin films.

#### 4. Conclusion

Thin films with good homogeneity can be successfully prepared from  $\text{Cu}_2\text{S}$  through chemical-bath method. Annealing exerted a clear effect on the structural properties of samples by increasing the crystallinity of thin films. Annealing also improved the electrical and optical properties of the prepared  $\text{Cu}_2\text{S}$  thin films in terms of increasing their  $\sigma$  and  $\alpha$ .

#### References

1. Osuwa J. C, Mgbaja E. C, "Effects of Mercury and Nickel Impurities on Optical Properties of Copper Sulfide ( $\text{Cu}_2\text{S}$ ) Thin Films Deposited by Chemical Bath Technique", IOSR Journal of Environmental Science, 5(2), 27-135, 2013.
2. IvanGrozdanov, MetodijaNajdoski, "Optical and Electrical Properties of Copper Sulfide Films of Variable Composition", Journal of Solid State Chemistry,(1995) 114(2), 469-475.
3. Huda Abdullah, Norhabibi Saada, Sahbuddin Shaari, "Effect of Deposition Time on ZnS Thin Film Properties by Chemical Bath Deposition (CBD) Technique", World Applied Sciences Journal, (2012) 9(8), 1087-1091.
4. Sartale, S. D, Lokhande, C. D, "Preparation and Characterization of Nickel Sulphide Thin Films Using Successive Ionic Layer Adsorption and Reaction (SILAR)", Material Chem. and Phys.,(2001) 72(8), 100-104.
5. J. Vedel, P. Cowache, M.Soubeyrand. "Electroplating of  $\text{Cu}_x\text{S}$  on  $\text{CdS}$ ", Solar Energy Materials, (1984), 10(1), 25-34.
6. Martinuzzi S., Sarti D., Vassilevski D., Zapien-Nataren, F., "Photodetection Properties of  $\text{Cu}_2\text{S}$ - $\text{CdS}$  Heterojunction Solar Cells", Solar Cells,(1980), 2,173-184.
7. L. Soriano, M. Leon, F. Arjona, E. Garcia Camarero, "On the Photoconductivity of Copper

- Sulphide Polycrystalline Thin Films**”, Solar Energy Materials, (1985), 12(2), 149-155.
8. Luminita Isaca, Ionut Popovicia, Alexandru Enescaa, Anca Dutaa,” **Copper Sulfide ( $\text{Cu}_x\text{S}$ ) Thin Films as Possible p-Type Absorbers in 3D Solar Cells**”, Energy Procedia, (2010),2, 71–78.
9. R.Suárez, P.K.Nair<sup>1</sup>, “**Co-Deposition of PbS–CuS Thin Films by Chemical Bath Technique**”, Journal of Solid State Chemistry,(1996), 123(2), 296-300.
10. J. C. Osuwa, E. C. Mgbaja, “**Structural and Electrical Properties of Copper Sulfide (CuS) Thin Films doped with Mercury and Nickel impurities**”, IOSR Journal of Applied Physics (2014), 6(5), 28-31.
11. Í. A. Kariper, “**Amorphous Pbse Thin Film Produced By Chemical Bath Deposition at pH of 5–8**”, Surface Review and Letters,(2020), 27(4), 1950128(1-5).
12. B. D. Cullity and S.R. Stock, “**Elements of X – Ray Diffraction**”, 3th edition, Prentice-Hall in the United States of America, 2001.
13. Shaji Varghese, Mercy Iype, “**Effect of Annealing on the Activation Energy of Thin Films of Manganese Sulphide, Copper Phthalocyanine and Multilayer Manganese Sulphide-Copper Phthalocyanine from their Electrical Studies**”, Oriental Journal of Chemistry,(2011), 27 (1), 265-269.
14. Bourbatache Mansour, Hanan Shaban, Samia A Gad, Yasser El-Gendy, Abdel-Badeeh M. Salem, “**Effect of Film Thickness, Annealing and Substrate Temperature on the Optical and Electrical Properties of  $\text{CuGa}_{0.25}\text{In}_{0.75}\text{Se}_2$  Amorphous Thin Films**”, Journal of Ovonic Research, (2010) 6(1), 13-22.
15. Olaf Stenzel, “**The Physics of Thin Film Optical Spectra: An Introduction**”, Springer Science & Business Media, 2005.
16. S. D. Hutagalwng, B. Y. Lee. Proceeding of the 2nd International conference, “**Nano/Micro Engineered and Molecular Systems**”, January Bangkok , Thailand, 2007.
17. Hans Kuzmany, “**Solid-State Spectroscopy: An Introduction**”, Springer Science & Business Media, Mar 9, 2013
18. A. Bediaa, F.Z. Bediaa, M. Ailleriea, N. Maloufid , B. Benyoucef, “**Influence of the Thickness on Optical Properties of Sprayed ZnO Hole-Blocking Layers Dedicated to Inverted Organic Solar Cells**”, Energy Procedia, (2014) 50, 603 – 609.